Multi-channel receiver module for IR wireless link

Lijun Jiang, New Wei Lee, Shiqian Wu, Rahardia Susanto
Laboratories for Information Technology (LIT), 21, Heng Mui Keng Terrace, Singapore 119613

A multi-channel auto-gain controllable receiver module for a 40Mbit/s LED based non-directed infrared wireless link is implemented using photodiode array followed by multi-channel transimpedance-summer architecture, band-pass filter, AGC, with EM shielding. It can receive signal with BER of 10^{-4} at 2 m vertically from the transmitter ±50° off the vertical axis.

Key words: **Receiver, noise figure, wireless communication.**

1 Introduction Short-range indoor wireless communication is playing more important role with the emergence of portable computing and multimedia terminals in work and living environment. Infrared technology is competent choice due to its good security in the room, large bandwidth and no need of regulations. Many indoor communication systems developed employ laser diode (LDs) as light source[1] [2]. Comparing with LD, light-emitting diode (LED) is inexpensive, and generally considered eye-safe. An infrared LED array-based wireless link has been built and its receiver module detailed in this paper is capable of receiving a 40Mbit/s on-off coding signal from a transmitter 2 meters away (Fig1).

2 Non-directed Infrared Wireless link system The infrared wireless link comprises a LED-based transmitter with peak spectral sensitivity of 870 nm and a receiver module. The LED-based transmitter uses special titling and orienting scheme to cover a field of ±50° with uniform power distribution. To receive the low power signal from LED based transmitter, an enhanced receiver module with shielding structure is built, consisting of a photo detector array followed by multi-channel transimpedance summer, band pass filters, auto-gain control unit (AGC). It should be able to achieve bit error rate (BER) of 10^{-4}.

3 Receiver module The minimum power required to achieve SNR = 1 at the detector for system bandwidth of 1 MHz to 20 MHz is 0.0309 μW, hence the highest possible SNR at input stage is 15.1004 dB. The SNR required at the output for BER = 10^{-4} is 11.3992 dB for on-off signal. Thus, the Noise Figure for the system must be less than 3.7012 dB. High speed PIN photodiode with ±60° half looking angle and peak response at 880 nm is selected as photo detector to ensure the low loss of power between the transmitter and receiver and good rejection of noise in other wavelength.
The trade-off between transit rise time and effective area make a large area photodiode slower speed of response. Cascading many photodiodes in parallel will increase capacitance. In our design, a multi-channel receiver architecture is designed and implemented (Fig2). In transimpedance amplifier, high load

resistance R_L looking from photodiode is desirable for high gain, but it reduces the bandwidth of the circuit. To make sure the circuit rise time to be insignificant to response speed of photodiode, i.e. being less than ¼ transit rise time of photodiode, R_L is found to be less than 114.16 and the subsequent feedback resistance R_f to be less than 1223.73 Ω for a CLC425 based transimpedance amplifier. Its slew rate of 350 V/μs is sufficient for operation of 20 MHz 4V pp modulating frequency. To eliminate the harmonics up to tens to hundreds of kilohertz [3] caused by fluorescent lamps emissions, a band-pass high-gain Sallen-Key 2nd order active filter with bandwidth of {1MHz 20MHz} is built.

For photodiode, it is desirable to have large effective area to collect as much power as possible. However, since transit rise time is proportional to the depletion width, usage of a large area photodiode necessarily means a slower speed of response. Photo-detector we used (BPW34FA) has a small radiant sensitive area of 7-mm^2 and a detector capacitance of 15 pF (biased at 10 V). Though cascading many photodiodes directly in parallel will help enlarge effective area, it also multiplies equivalent capacitance. To resolve this problem, a multi-channel architecture isolating each detector-preamplifier channel and then summing up the voltages of each channel up is designed and implemented. A noise figure (NF) - channel number model of the multi-channel amplifier-summer architecture is built up based on input voltage and current noise density and a simulation is done to determine the optimal numbers of channels. In view the simulation results (Fig. 4) that show that there is little improvement in NF once channel numbers > 10, 10 channels is chosen. Although small R_f gives lower NF, it produces smaller phase margin to make system unstable. To have a phase margin of more than 60°, 20 log(R_f) must be equal to 60 dB, giving a minimum R_f equal to 1000 Ω. Followed the summer is a 2-stage amplifier to give a maximum current-to-voltage gain of 113.98 dB. Amplification at this stage should not give a high voltage as the active filters followed have gain too and overdriving the input of the active filters will give distortions to signals. Using together with a 1pF shunt capacitance, feedback resistance is set to be large enough (>1000 Ω) to ensure a phase margin of more than 70° to make the system stable.

Due to the fluctuation of incident light caused by partial obstruction to the photodiode, it is necessary to stabilize the signal. An auto-gain control (AGC) unit is designed using amplifier with voltage controlled gain and inverting integrator configuration in a feedback loop. The testing results are shown in Fig3**.** The AGC effect is relative constant for input to the AGC from a range of 0.4 V to 2 V.

The high gain receiver has to be immune to electromagnetic interference. A aluminum alloy die-cast box of thickness 2 mm with 630.4 dB shielding effectiveness (SE) at 10MHz offered good attenuation of radiation sources. A copper board having a window aperture of 10 cm by 8 cm screened by wire mesh is used as top cover. Using the maximum spacing of 10mm, SE of the screen mesh is 64 dB and 58.0 dB for 10 MHz and 20 MHz respectively. However, this attenuation is not good enough for frequencies in the range {15 MHz 18 MHz}. To overcome the inadequacies of the shielded box, a metal box with the shape of waveguide is inserted on top of the aperture to better attenuate the EM signal.

Intersymbol interference (ISI) caused in diffused infrared systems is dependent on the room size and bit rate. ISI might become substantial with growing severity from 30 Mbps. The method to overcome ISI is to use a digital equalizer element as part of the digital signal processing (DSP) circuits in the receiver. Our receiver does not incorporate an equalizer as part of the design as it operates in a relative small room (3.4m x 5.1m x 2.6m) at maximum 40 Mbps rate.

4 Results A digital transmission analyzer (DTA) operated at 40 Mbps with on off coding signals drives the infrared LED based transmitter mounted on the ceiling in a testing room with light on. Receiver was placed at vertical separation of 1.98 m from the transmitter and signals were collected at different angles from vertical axis of transmitter. Signals obtained from the receiver were fed to the DTA and digital Sampling Oscilloscope for BER testing and eye diagram respectively. The eye diagrams obtained for "10101010 10101010 " is shown in Figure 5. The BER obtained for 3 different codes "11000-10110110001", "1101011010100010", and "1101000101100010" at different offset angel was shown in Figure 6. Further BER improvement up to10^{-5}~10^{-6} can be achieved by positioning a convex lens above the photodiodes.

5 Conclusions

An auto gain controllable receiver module has been established which can operate at 40 Mbit/s for a non-directed LED-based infrared wireless link. Photodiode arrays with multi-channel processing give large signal collection area while providing high speed of response. This work demonstrates the feasibility of construction a high speed, inexpensive and eye-safe short-range infrared communication link.

Acknowledgment: This work was supported by Singapore "R&Bnet at Home" project.

References

[1] M. J MacCullagh, '155 Mbit/s optical wireless link using a bootstrapped silicon APD receiver ', Electronic Letters, 1994, 30(5), pp.430-432,

[2] G. W. Marsh and J. M.Kahn, 'Performance Evaluation of Experimental 50-Mbps Diffuse Infrared Wireless Link using On-Off Keying with Decision-Feedback Equalization', IEEE Trans on Comm, 1996, 44(11), pp.1496-1504

[3] J. M. Kahn and J. R. Barry, 'Wireless Infrared Communications', Proc IEEE, 1997, 85(3), pp.265-298.

Figure Captions

Fig. 1 Schematic diagram of wireless IR link

Fig. 2 Block diagram of receiver module

Fig. 3 AGC results at two frequencies

Fig. 4 Variation of noise figure with number of channels

Fig. 5 Eye diagram for "10101010 10101010"

Fig. 6 BER variation with offset angle at 40Mbit/s

Figure 1

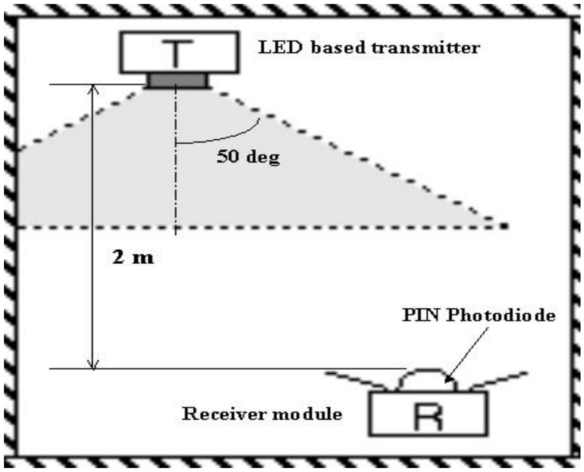

Figure 2

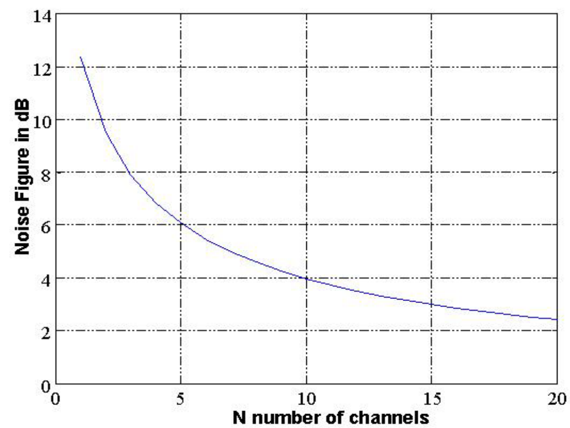

Figure 5

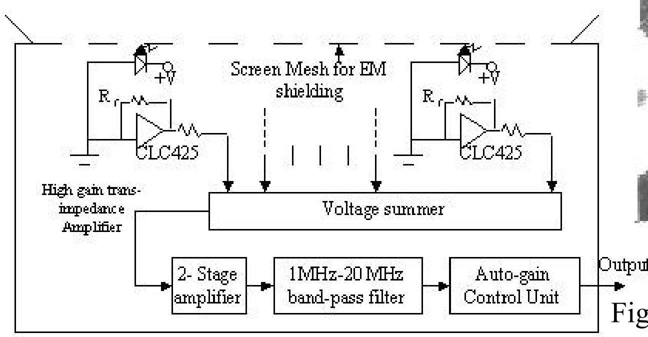

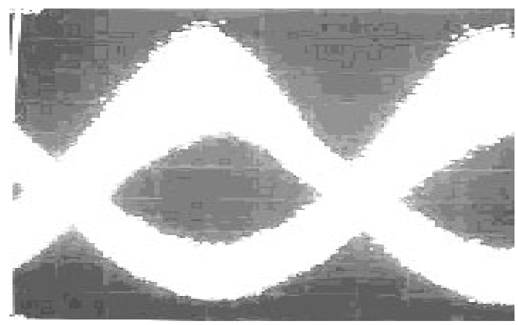

Figure 6

Figure 3

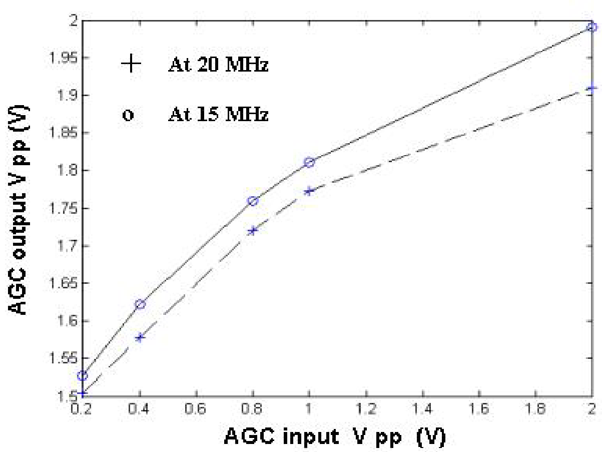

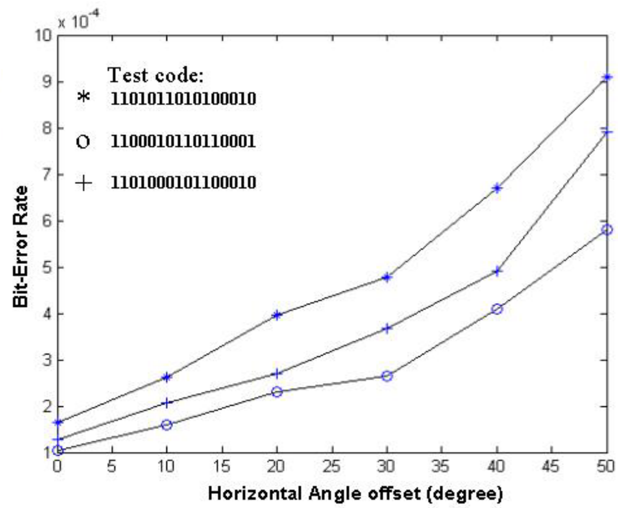

Figure 4